Synthesis and Characterization of Novel Fluorinated Polyimides Based on 2,7-Bis(4-amino-2-trifluoromethylphenoxy)naphthalene

SHENG-HUEI HSIAO, CHIN-PING YANG, CHENG-LIN CHUNG

Department of Chemical Engineering, Tatung University, 40 Chungshan North Road, Section 3, Taipei 104, Taiwan, Republic of China

Received 29 January 2003; accepted 14 April 2003

ABSTRACT: A new trifluoromethyl-substituted bis(ether amine) monomer, 2,7-bis(4-amino-2-trifluoromethylphenoxy)naphthalene, was synthesized. It led to a series of novel fluorinated polyimides by thermal and chemical imidization routes when reacted with various commercially available aromatic tetracarboxylic dianhydrides. Most of the polyimides obtained from both routes were soluble in many organic solvents, such as *N,N*-dimethylacetamide. All the polyimides could afford transparent, flexible, and strong films with low moisture absorptions of 0.3–0.6%, low dielectric constants of 2.52–3.27 at 10 kHz, and an ultraviolet–visible absorption cutoff wavelength at 377–436 nm. The glass-transition temperatures of the polyimides were in the range of 244–297 °C, and the 5% weight-loss temperatures were higher than 550 °C. For a comparative study, a series of analogous polyimides based on 2,7-bis(4-aminophenoxy)naphthalene were also prepared and characterized. © 2003 Wiley Periodicals, Inc. J Polym Sci Part A: Polym Chem 41: 2001–2018, 2003

Keywords: trifluoromethyl; fluorinated polyimides; fluoropolymers; solubility; thermal properties; optical transparency; low dielectric constants; structure-property relations

INTRODUCTION

Aromatic polyimides have widely been used in electronic packaging applications because of their excellent thermal, mechanical, and electrical properties.[1] However, polyimides have one major drawback, their intractability in their fully imidized form. Therefore, polyimide processing is generally carried out from poly(amic acid) solutions that are cast into films and then subjected to a rigorous thermal treatment that converts the poly(amic acid) into polyimide. This method is well understood, but it has some inherent problems, such as the storage instability of the poly(amic acid) and the release of volatile byproducts (e.g., water) during imidization. For such difficulties to be overcome, polymer structure modification becomes necessary. Much success has been achieved in designing and synthesizing new dianhydrides[2–10] and diamines,[11–17] and so a great variety of soluble and processable polyimides have been produced for various purposes.

A low dielectric constant is one of the most attractive properties of polyimide materials for microelectronics applications. For a polymer structure to be achieved with a low dielectric constant, repeating units with low polarity and low polarizability have to be used.[18] This also reduces the moisture uptake. For example, the incorporation of an aliphatic adamantane or diamantane

Correspondence to: S.-H. Hsiao (E-mail: shhsiao@ttu.edu.tw)

Journal of Polymer Science: Part A: Polymer Chemistry, Vol. 41, 2001–2018 (2003)

moiety is known to result in low dielectric constants because of the high hydrophobicity, low polarity, and increased free volume.[19–22] It is also well known that the incorporation of fluorinated substituents into polymers reduces the dielectric constant because of the low electronic polarizability of the C—F bond and the increase in the fractional free volume, which accompanies the replacement of methyl groups by trifluoromethyl (CF_3) groups. Therefore, fluorinated polyimides were developed to reduce the dielectric constant.[23–27] An additional positive effect of fluorinated substituents is to enhance the solubility and optical transparency of polyimides.

Recent studies have demonstrated that polyimides derived from ether-bridged aromatic diamines with CF_3 substituents are soluble, high-temperature polymer materials with low moisture uptake, low dielectric constants, and high optical transparency.[28–38] The CF_3-substituted bis(ether amine) building blocks can, for example, be synthesized by the condensation of aromatic diols with 2-chloro-5-nitrobenzotrifluoride followed by reduction. This strategy allows the use of any sufficiently nucleophilic aromatic diol for the synthesis and, therefore, opens up the path to a large number of CF_3-substituted bis(ether amine)s. In previous publications,[39–43] we reported the synthesis of several naphthalene-based bis(ether amine)s, such as 1,4-, 1,5-, 1,6-, 1,7-, 2,3-, and 2,7-bis(4-aminophenoxy)naphthalenes (BAPONs) and their derived polyimides. However, apart from some soluble polymers derived from 2,3-BAPON, most of the polyimides based on other naphthalene residues have limited solubilities. As part of our continuing efforts in developing tractable high-performance polymers bearing naphthalene units, this work describes the successful synthesis of a new CF_3-substituted bis(ether amine), 2,7-bis(4-amino-2-trifluoromethylphenoxy)naphthalene (**2**), and its use for the preparation of soluble polyimides by the reaction of the diamine with dianhydrides. The polymers were subjected to solubility tests and thermal, optical, and dielectric property measurements and were compared to analogous counterparts prepared from a structurally similar, nonfluorinated bis(ether amine), 2,7-BAPON. The fluorine-containing polyimides were expected to exhibit enhanced solubility and diminished dielectric constants because of the increased free volume caused by the CF_3 groups.

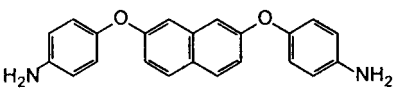

2,7-BAPON

EXPERIMENTAL

Materials

2,7-Dihydroxynaphthalene (Tokyo Chemical Industry), potassium carbonate (K_2CO_3; Fluka), 2-chloro-5-nitrobenzotrifluoride (Acros), *p*-chloronitrobenzene (Acros), 10% palladium on charcoal (Pd/C; Fluka), and hydrazine monohydrate (Acros) were used as received. According to a literature procedure,[39–43] 2,7-BAPON (mp = 172–173 °C) was prepared by the aromatic nucleophilic substitution reaction of 2,7-dihydroxynaphthalene with *p*-chloronitrobenzene in the presence of K_2CO_3 and the subsequent reduction of the intermediate dinitro compound with hydrazine as the reducing agent and palladium as the catalyst. Commercially available aromatic tetracarboxylic dianhydrides such as pyromellitic dianhydride (PMDA or **3a**; Aldrich), 3,3′,4,4′-benzophenonetetracarboxylic dianhydride (BTDA or **3c**; Aldrich), 3,3′,4,4′-diphenylsulfonetetracarboxylic dianhydride (DSDA or **3d**; New Japan Chemical Co.), and 4,4′-oxydiphthalic dianhydride (ODPA or **3e**; Oxychem) were purified by recrystallization from acetic anhydride. 3,3′,4,4′-Biphenyltetracarboxylic dianhydride (BPDA or **3b**; Oxychem) and 2,2-bis(3,4-dicarboxyphenyl)hexafluoropropane dianhydride (6FDA or **3f**; Hoechst Celanese) were purified by vacuum sublimation. *N,N*-Dimethylacetamide (DMAc) was purified by distillation under reduced pressure over calcium hydride and stored over 4-Å molecular sieves.

Monomer Synthesis

2,7-Bis(2-trifluoromethyl-4-nitrophenoxy)-naphthalene (1)

2,7-Dihydroxynaphthalene (8.0 g, 0.05 mol) and 2-chloro-5-nitrobenzotrifluoride (23.0 g, 0.10 mol) were dissolved in 100 mL of dimethyl sulfoxide (DMSO) in a 300-mL, round-bottom flask. Then, K_2CO_3 (14.0 g, 0.10 mol) was added, and the suspension mixture was heated at 100 °C for 8 h. The mixture was allowed to cool and then was poured into 600 mL of water to give a yellow solid, which was collected, washed repeatedly with wa-

ter, and dried. The crude product was recrystallized from methanol/water to give pale-yellow crystals [20.9 g, 78%; mp = 123–124 °C (onset to the peak top temperature) according to differential scanning calorimetry (DSC) at a scan rate of 2 °C/min].

IR (KBr): 1527, 1353 (—NO_2), 1240 (C—O stretch), 1138 cm^{-1} (C—F stretch). ^1H NMR ($CDCl_3$, δ, ppm): 8.59 (d, J = 2.7 Hz, 2H, H_f), 8.32 (dd, J = 9.1, 2.7 Hz, 2H, H_e), 8.02 (d, J = 9.0 Hz, 2H, H_c), 7.52 (d, J = 2.4 Hz, 2H, H_a), 7.31 (dd, J = 9.0, 2.4 Hz, 2H, H_b), 7.04 (d, J = 9.1 Hz, 2H, H_d). ^{13}C NMR ($CDCl_3$, δ, ppm): 160.6 (C^7), 153.2 (C^3), 142.2 (C^{10}), 135.3 (C^1), 131.1 (C^5), 129.3 (C^6), 128.9 (C^9), 123.1 (quartet, $^3J_{C—F}$ = 5 Hz, C^{11}), 122.2 (quartet, $^1J_{C—F}$ = 277 Hz, C^{13}), 121.1 (quartet, $^2J_{C—F}$ = 30 Hz, C^{12}), 120.1 (C^8), 117.9 (C^2), 116.9 (C^4).

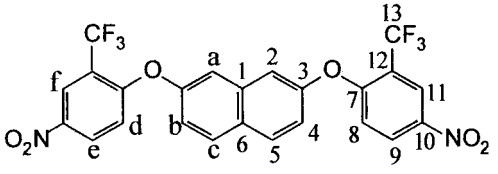

Crystal data: pale-yellow crystal grown during slow crystallization in methanol/water (1:1 v/v), 0.40 mm × 0.35 mm × 0.35 mm, triclinic P-1 with a = 8.12060(10), b = 10.97220(10), c = 13.7619(2) Å, α = 112.3040(10), β = 94.8960(10), and γ = 96.0690(10)°, where D_C (the density of crystal) = 1.600 mg/m^3 for Z = 2 and volume (V) = 1117.56(2) $Å^3$. ELEM. ANAL. Calcd for $C_{24}H_{12}F_6N_2O_6$ (538.36): C, 53.54%; H, 2.24%; N, 5.20%. Found: C, 53.68%; H, 2.30%; N, 5.29%.

2,7-Bis(4-amino-2-trifluoromethylphenoxy)naphthalene (2)

A mixture of the purified dinitro compound **1** (16.0 g, 0.03 mol), 10% Pd/C (0.15 g), ethanol (100 mL), and hydrazine monohydrate (10 mL) was heated at the reflux temperature for about 8 h. The resultant clear, darkened solution was filtered hot to remove Pd/C, and the filtrate was then distilled to remove the solvent. The crude product was purified by recrystallization from ethanol/water to give pale-yellow (almost colorless) crystals (10.6 g, 75%; mp = 161–162 °C according to DSC at 2 °C/min).

IR (KBr): 3485, 3453, 3372 (N—H stretch), 1220 (C—O stretch), 1123 cm^{-1} (C—F stretch). ^1H NMR ($CDCl_3$, δ, ppm): 7.72 (d, J = 8.9 Hz, 2H, H_c), 7.11 (dd, J = 8.9, 2.3 Hz, 2H, H_b), 6.95 (d, J = 2.3 Hz, 2H, H_a), 6.94 (d, J = 2.6 Hz, 2H, H_f), 6.87 (d, J = 8.7 Hz, 2H, H_d), 6.74 (dd, J = 8.7, 2.6 Hz, 2H, H_e), 3.72 (s, 4H, —NH_2). ^{13}C NMR ($CDCl_3$, δ, ppm): 157.3 (C^3), 145.7 (C^7), 143.1 (C^{10}), 135.5 (C^1), 129.8 (C^5), 126.5 (C^6), 123.5 (quartet, $^2J_{C—F}$ = 30 Hz, C^{12}), 123.4 (quartet, $^1J_{C—F}$ = 277 Hz, C^{13}), 123.4 (C^8), 119.6 (C^9), 117.7 (C^2), 113.2 (quartet, $^3J_{C—F}$ = 5 Hz, C^{11}), 117.6 (C^4).

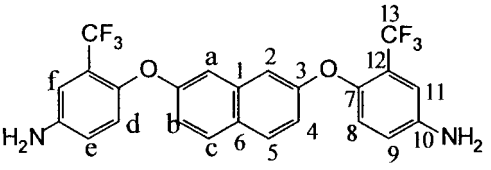

Crystal data: almost colorless crystal grown during slow crystallization in ethanol/water (4:1 v/v), 0.35 mm × 0.30 mm × 0.25 mm, orthorhombic $P2_12_12_1$ with a = 8.45600(10), b = 10.23300(10), c = 25.3450(4) Å, α = 90, β = 90, and γ = 90°, where D_C = 1.449 mg/m^3 for Z = 4 and V = 2193.11(5) $Å^3$. ELEM. ANAL. Calcd for $C_{24}H_{16}F_6N_2O_2$ (478.39): C, 60.26%; H, 3.37%; N, 5.85%. Found: C, 60.39%; H, 3.53%; N, 5.94%.

Polymer Synthesis

The polyimides were synthesized from various dianhydrides and diamine **2** via a two-step method. The synthesis of polyimide **5f** is used as an example to illustrate the general synthetic route used to produce the polyimides. To a solution of 0.3632 g (1.01 mmol) of **2** in 9.5 mL of CaH_2-dried DMAc in a 50-mL flask, 0.6368 g (1.01 mmol) of dianhydride 6FDA was added in one portion. Therefore, the solid content of the solution was approximately 10 wt %. The mixture was stirred at room temperature overnight (for ca. 12 h) to afford a highly viscous poly(amic acid) solution. The inherent viscosity of the resulting poly(amic acid) (**4f**) was 0.98 dL/g, measured in DMAc at a concentration of 0.5 g/dL at 30 °C. The poly(amic acid) was subsequently converted into polyimide by either a thermal or chemical imidization process. For the thermal imidization process, about 7 g of the obtained poly(amic acid) solution was poured into a 9-cm glass culture dish, which was placed overnight in a 90 °C oven for the slow release of the casting solvent. The semidried poly(amic acid) film was further dried and transformed into polyimide **5f** by sequential

heating at 150 °C for 30 min, 200 °C for 30 min, and 250 °C for 1 h. The polyimide film was stripped from the glass substrate by being soaked in water. The inherent viscosity of **5f** was 0.76 dL/g in DMAc at a concentration of 0.5 g/dL at 30 °C. For the tensile testing, dielectric constants, and thermogravimetric analysis (TGA), the polyimide films were further heated at 300 °C for another 1 h. Chemical imidization was carried out via the addition of 2 mL of pyridine and 5 mL of acetic anhydride into the remaining poly(amic acid) solution at room temperature overnight. The resulting homogeneous polyimide solution was poured into methanol to give a light yellow, fibrous precipitate, which was collected by filtration, washed thoroughly with methanol, and dried.

Measurements

Elemental analyses were run in a PerkinElmer model 2400 CHN analyzer. IR spectra were recorded on a PerkinElmer Spectrum GX Fourier transform infrared (FTIR) system. ^{1}H and ^{13}C NMR spectra were measured on a JEOL EX 400 spectrometer with $CDCl_3$ as the solvent and tetramethylsilane as the internal reference. The X-ray crystallographic data were collected on an Enraf-Norius FR 590 CAD-4 diffractometer. The inherent viscosities of the polymers were measured with an Ubbelohde viscometer at 30 °C. Wide-angle X-ray diffraction (WAXD) measurements were performed at room temperature (ca. 25 °C) on a Shimadzu XRD 6000 X-ray diffractometer (40 kV and 20 mA) with graphite-monochromatized Cu Kα radiation. Gel permeation chromatography (GPC) was carried out on a Waters chromatography unit interfaced with a Waters 2410 refractive-index detector. Two Waters 5-μm Styragel HR-2 and HR-4 columns (7.8-mm inside diameter $\times$ 300 mm) connected in series were used with tetrahydrofuran (THF) as the eluent and were calibrated with narrow polystyrene standards. An Instron universal tester (model 1130) with a load cell of 5 kg was used to study the stress–strain behavior of the polyimide film samples. A gauge length of 2 cm and a crosshead speed of 5 mm/min were used for this study. The measurements were performed at room temperature with film specimens (0.5 cm wide, 6 cm long, and ca. 0.09 mm thick), and an average of at least five individual determinations was used. The color intensity of the polymers was evaluated with a Macbeth color-eye colorimeter. The measurements were performed with films (83–93 μm thick) with an observational angle of 10° and a Commission International de l'Eclairage (CIE)-D illuminant. A CIE LAB color difference equation was used. Ultraviolet–visible (UV–vis) spectra of the polymer films were recorded on a Shimadzu UV-1601 UV–vis spectrophotometer. The dielectric property of the polymer films was tested by the parallel-plate capacitor method with an HP-4194A impedance/gain phase analyzer. Gold electrodes were vacuum-deposited onto both surfaces of dried films. Experiments were performed at 25 °C in a dry chamber. TGA was conducted with a PerkinElmer Pyris 1 TGA. Experiments were carried out on approximately 6–8-mg film samples heated in flowing nitrogen or air (flow rate = 30 cm^3/min) at a heating rate of 20 °C/min. DSC analyses were performed on a PerkinElmer Pyris 1 DSC at a scan rate of 20 °C/min in flowing nitrogen (20 cm^3/min). Glass-transition temperatures (T_g's) were read at the middle of the transition in the heat capacity and were taken from the second heating scan after quick cooling from 400 °C at a cooling rate of 200 °C/min. Thermomechanical analysis (TMA) was conducted with a PerkinElmer TMA 7 instrument. The TMA experiments were conducted from 50 to 300 °C at a scan rate of 10 °C/min with a penetration probe 1.0 mm in diameter under an applied constant load of 10 mN. Softening temperatures (T_s's) were taken as the onset temperatures of probe displacement on the TMA traces. The equilibrium moisture absorption was determined by the weighing of the changes in vacuum-dried film specimens before and after immersion in deionized water at 25 °C for 3 days.

RESULTS AND DISCUSSION

Monomer Synthesis

The new CF_3-containing bis(ether amine) **2** was prepared in two steps according to a well-developed method,[11,12] as shown in Scheme 1. The first step was a Williamson etherification of 2,7-dihydroxynaphthalene with 2-chloro-5-nitrobenzotrifluoride in the presence of K_2CO_3 in DMSO. **2** was readily obtained in high yields by the catalytic reduction of intermediate dinitro compound **1** with hydrazine hydrate and Pd/C catalyst in refluxing ethanol. The structures of **1** and **2** were confirmed by FTIR, NMR, elemental, and X-ray crystal analysis. Figure 1 shows the FTIR spectra of dinitro compound **1** and diamine **2**. Absorption

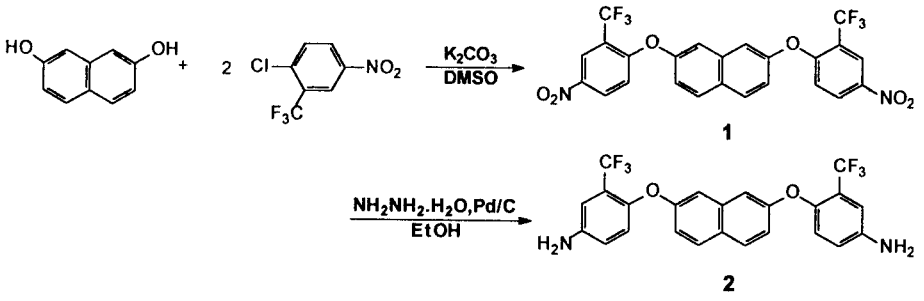

Scheme 1

bands representative of the nitro functionality were identified in the FTIR spectrum. The nitro group of **1** gave two characteristic bands at 1596 and 1353 cm^{-1} (NO_2 asymmetric and symmetric stretching). After reduction, the characteristic absorptions of the nitro group disappeared, and the amino group showed the typical N—H stretching bands in the region of 3300–3500 cm^{-1}. Figures 2 and 3 illustrate the ^1H NMR and ^{13}C NMR spectra of dinitro compound **1** and diamine **2**, respectively. The ^1H NMR spectra (Fig. 2) confirm that the nitro groups were completely converted into amino groups by the high field shift of the aromatic protons and by the signal at 3.72 ppm corresponding to the primary aromatic amine protons. Figure 3 presents the ^{13}C NMR spectra of dinitro compound **1** and diamine **2** in $CDCl_3$. All the carbon-13 atoms in dinitro compound **1** and 3F-diamine **2** resonated in the region of 110–160 ppm, and the ^{13}C NMR spectra of **1** and **2** show

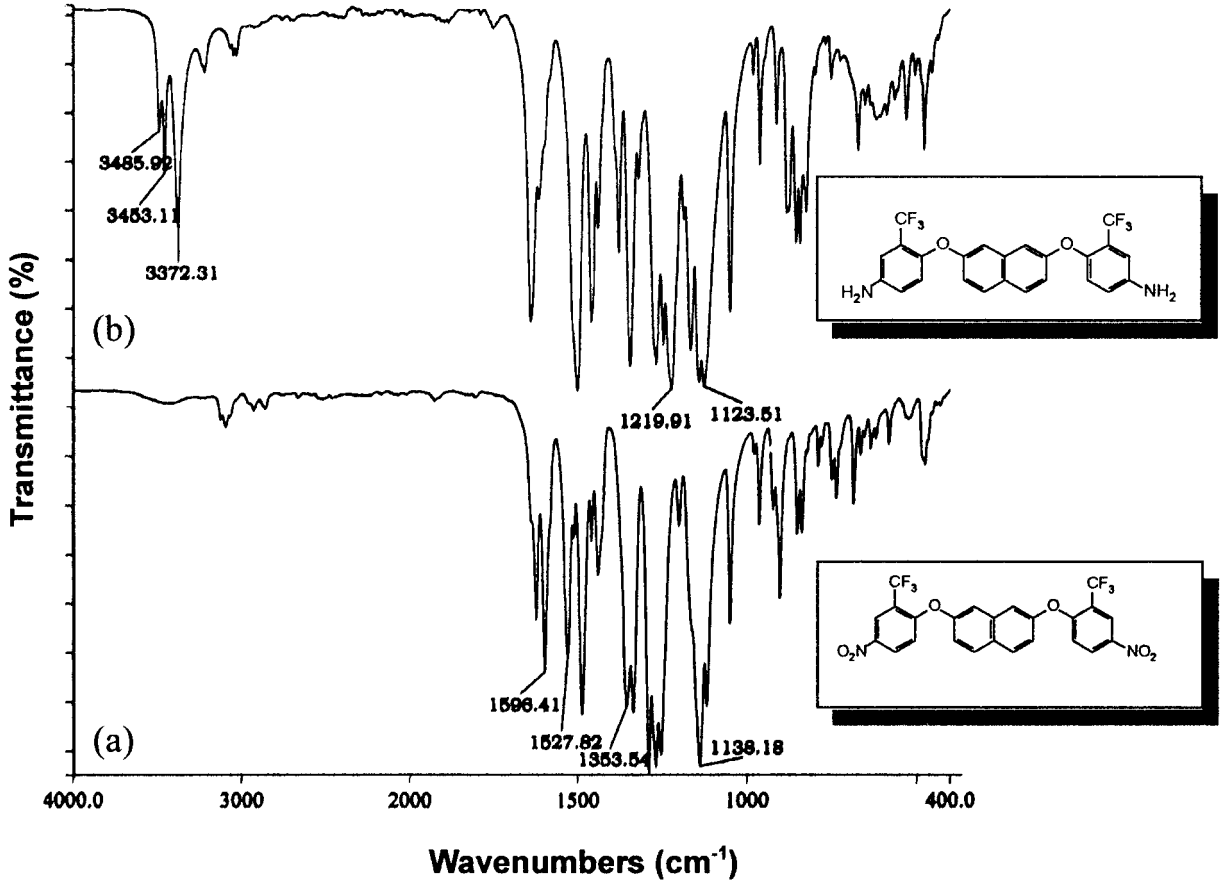

Figure 1. IR spectra of (a) dinitro compound **1** and (b) diamine **2**.

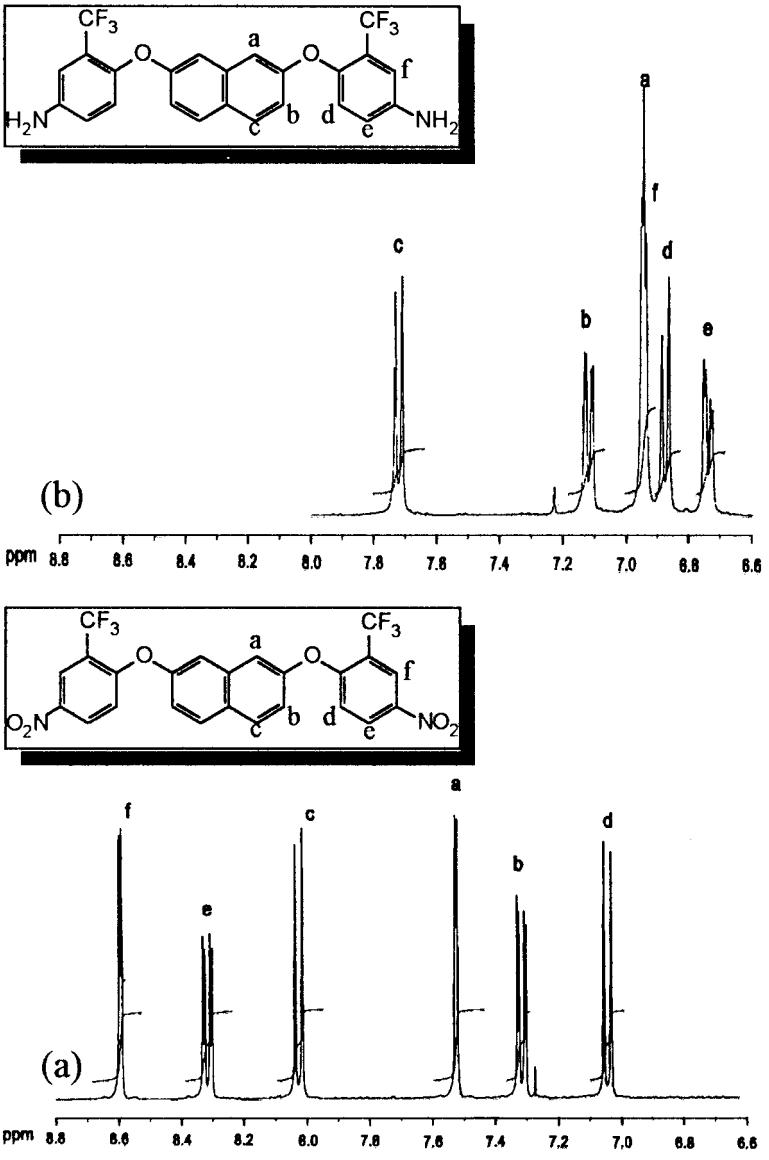

Figure 2. Expansions of the aromatic ring proton resonance from the 400-MHz ^1H NMR spectra of (a) dinitro compound **1** and (b) diamine **2** in $CDCl_3$. The accompanying amino group resonance (—NH_2 at 3.72 ppm) of **2** is not shown.

three quartets because of the heteronuclear ^{13}C–^{19}F coupling. The large quartets centered at about 122.2 ppm for **1** and at 123.4 ppm for **2** were due to the —CF_3 carbons. The one-bond C—F coupling constant in these cases was about 277 Hz. The CF_3-attached carbon C^{12} also showed a clear quartet centered at about 121.1 ppm for **1** and at 123.5 ppm for **2** with a smaller coupling constant of about 30 Hz due to two-bond C—F coupling. Besides, the C^{11} carbon (ortho to the CF_3 group) also had its resonance split by the three fluorines (three-bond coupling). The close quartet had an even smaller coupling constant (ca. 5 Hz) because the interaction operated over more bonds. Therefore, all the spectroscopic data obtained were in good agreement with the expected structures. The molecular structures of **1** and **2** were also confirmed by X-ray crystal analysis. X-ray crystal data for **1** and **2** were acquired from the single crystal obtained by slow crystallization of a methanol/water solution of **1** and an ethanol/water solution of **2**. As shown in Figure 4, compounds **1** and **2** displayed a bent structure, and the benzene and naphthalene rings were not in the same

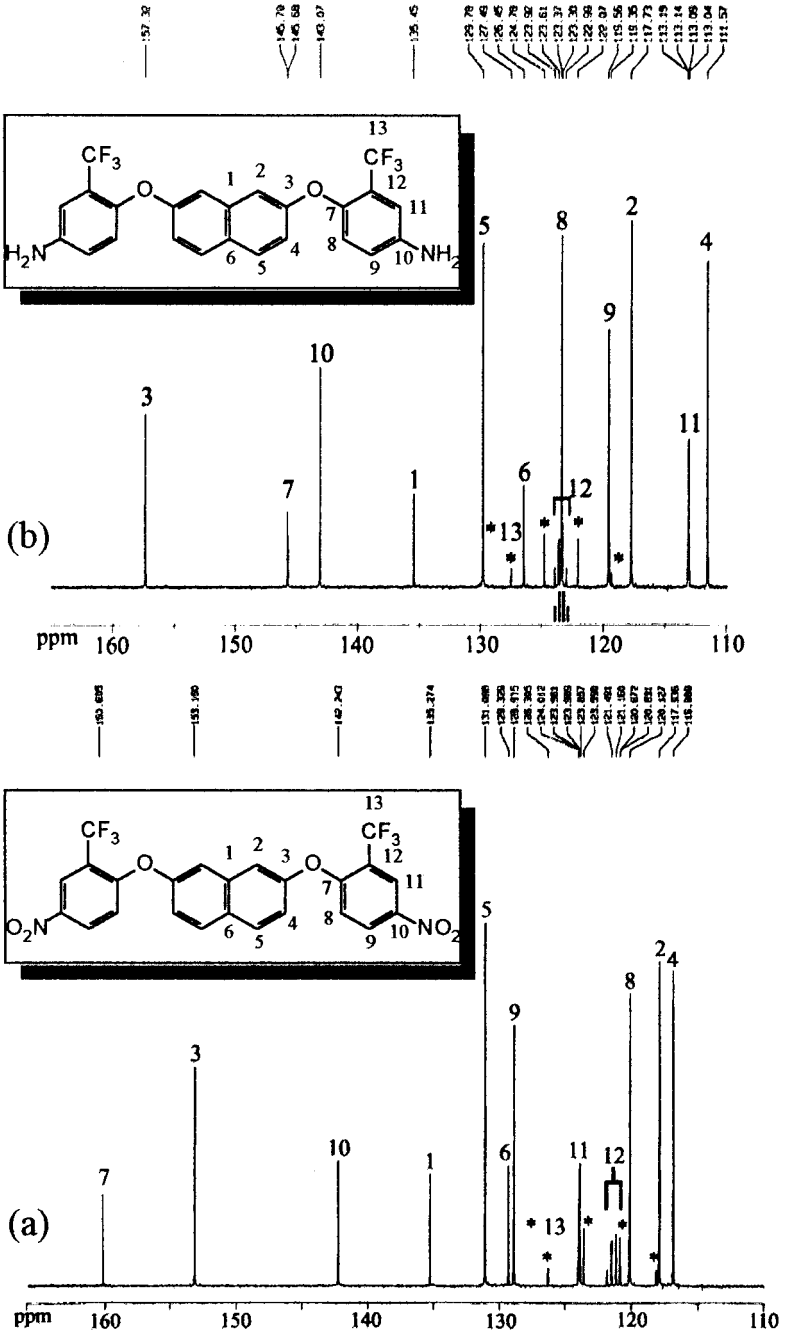

Figure 3. ^{13}C NMR spectra of (a) dinitro compound **1** and (b) diamine **2** in $CDCL_3$.

plane because of the serious CF_3 steric hindrance. This conformation hindered the close packing of polymer chains and enhanced the solubility of fluorinated polyimides.

Polymer Synthesis

The polyimides were prepared from diamine **2** and six commercially available dianhydrides (**3a**–**3f**) by a conventional two-step synthetic method shown in Scheme 2. Despite the presence of electron-withdrawing CF_3 substituents, **2** was still sufficiently reactive to give high molecular weight poly(amic acid)s when allowed to polymerize for a longer time (ca. 12 h). As shown in Table 1, the inherent viscosities of the intermediate poly(amic acid)s ranged from 0.79 to 1.27 dL/g. The molecular weights of all the poly(amic acid)s were suf-

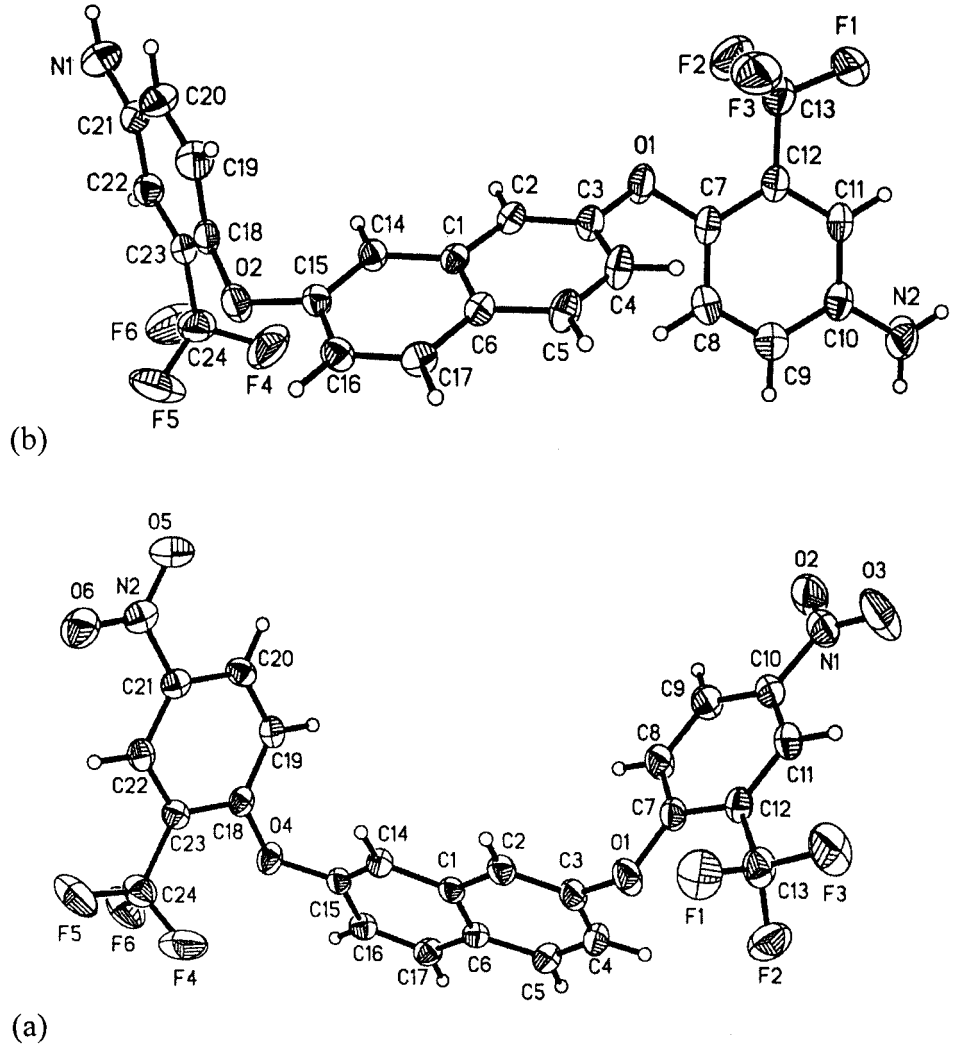

Figure 4. X-ray structures of (a) dinitro compound **1** and (b) diamine **2**.

ficiently high to permit the casting of flexible and tough poly(amic acid) films, which were subsequently converted into tough polyimide films by extended heating at elevated temperatures. **2** mostly likely retained its reactivity because it was meta to the CF_3 group. Some of the thermally cured polyimides exhibited excellent solubility in polar solvents such as *N*-methyl-2-pyrrolidone (NMP) and DMAc. Therefore, the characterization of the solution viscosity was carried out without any difficulty, and the inherent viscosities of the organosoluble polyimides were recorded in the range of 0.76–1.31 dL/g, as measured in DMAc at 30 °C. For a comparative study, a series of reference polyimides (**6a–6f**) were also synthesized from 2,7-BAPON and dianhydrides **3a–3f**. The inherent viscosities of the precursor poly(amic acid)s of **6a–6f** were in the range of 1.16–2.90 dL/g, indicating high molecular weight polymer formation. The chemically cyclodehydrated polyimides **5c–5f** exhibited inherent viscosities of 0.60–0.81 dL/g in DMAc, and their weight-average molecular weights (M_w's) and number-average molecular weights (M_n's) were recorded in the ranges of 61,000–86,500 and 38,000–52,500, respectively, relative to polystyrene standards (Table 2).

The formation of polyimides was confirmed with IR and elemental analysis. Figure 5 demonstrates a typical set of IR spectra for poly(amic acid) **4b** and polyimide **5b**. All the polyimides exhibited characteristic imide group absorptions around 1780 and 1725 cm^{-1} (typical of imide carbonyl asymmetrical and symmetrical stretch), 1380 cm^{-1} (C—N stretch), and 1100 and 730 cm^{-1} (imide ring deformation), together with

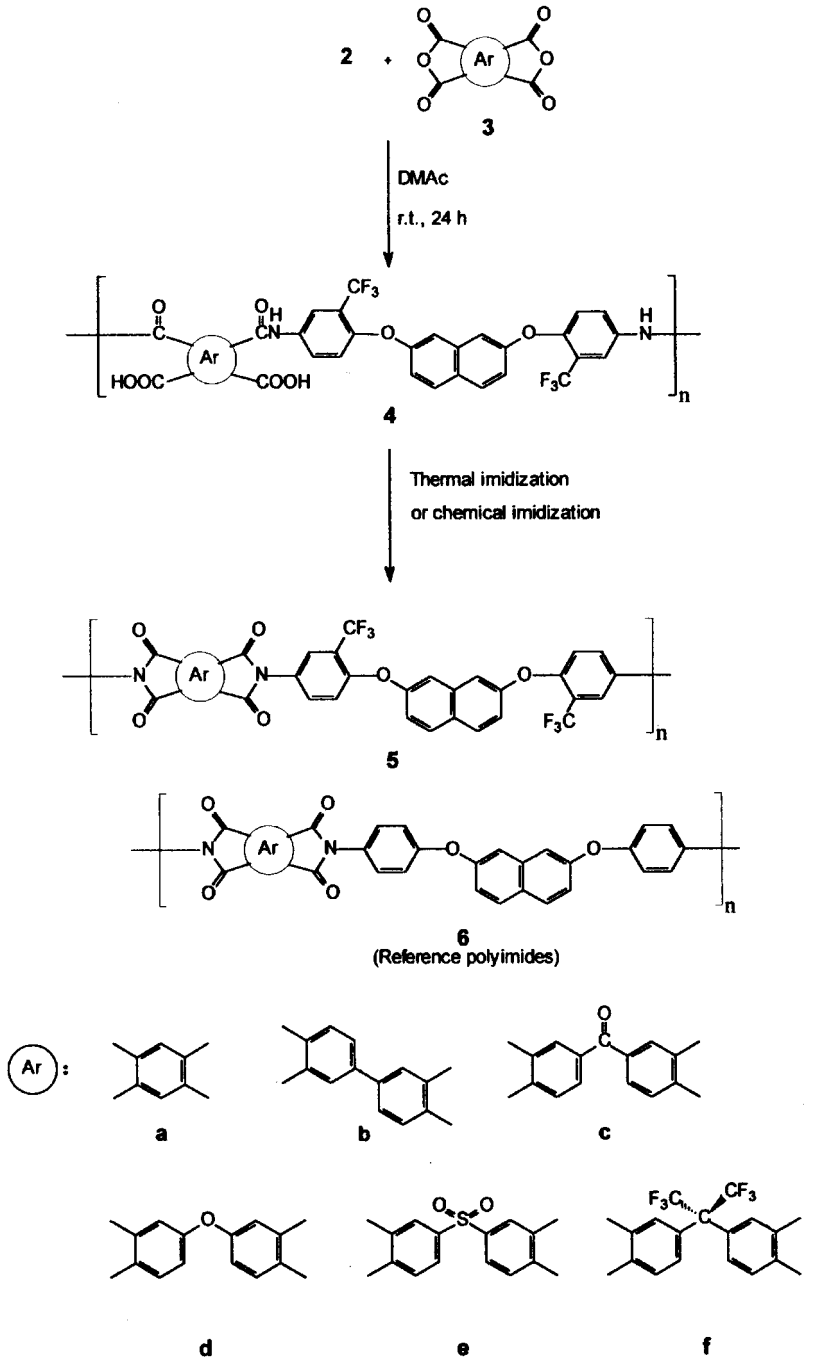

Scheme 2

some strong absorption bands in the region of 1100–1300 cm^{-1} due to the C—O and C—F stretching. The disappearance of amide and carboxyl bands indicated a virtually complete conversion of the poly(amic acid) precursor into polyimide. The results of the elemental analyses of all the thermally cured polyimides are listed in Table 3. The values found were in good agreement with the ones calculated for the proposed structures.

Polymer Properties

Organosolubility

The solubility of the polyimides was tested qualitatively in various organic solvents. The solubility properties of the thermally cured polyimides are reported in Table 4. All the **5** series polyimides, except for **5b**, exhibited good solubility, presumably because of the bulky pendant CF_3 group.

Table 1. Inherent Viscosity (η_{inh}) Values and Thin-Film Tensile Properties of the Polyimides Prepared via Thermal Imidization

Polyimide Code	η_{inh} of Poly(amic acid) (dL/g)[a]	η_{inh} of Polyimide (dL/g)[a]	Tensile Properties of the Polyimide Films		
			Tensile Strength (MPa)	Elongation to Break (%)	Initial Modulus (GPa)
5a	1.27	1.08	93	14	2.07
5b	0.82	—[b]	112	13	1.98
5c	0.79	—	112	9	2.00
5d	0.82	1.10	115	15	2.09
5e	0.89	1.31	94	8	2.02
5f	0.98	0.76	107	11	2.04
6a	2.90	—	97	24	2.01
6b	1.32	—	108	11	2.01
6c	1.46	—	117	8	2.32
6d	1.16	—	106	13	1.91
6e	1.92	—	116	10	2.37
6f	1.87	0.73	112	11	2.22

[a] Measured at a polymer concentration of 0.5 g/dL in DMAc at 30 °C.
[b] Insoluble in DMAc.

The thermally cured polyimides at 250 °C were soluble in strong dipolar solvents, such as NMP, DMAc, *N,N*-dimethylformamide (DMF), and DMSO, and phenol solvents, such as *m*-cresol and 2-chlorophenol. The polyimides (**5d**–**5f**) derived from less stiff dianhydride components were also soluble in common organic solvents such as THF, 1,4-dioxane, dichloromethane, and acetone. In some cases, the polymers became partly soluble or insoluble after curing at 300 °C, and this is possibly attributable to the fact that a molecular weight healing process or compact aggregation of the polymer chains occurred as imidization was carried out at a higher temperature. Conversely, for the **6a**–**6f** series, only polyimide **6f**, derived from 6FDA, displayed good solubility. Poor solubility for the **6** polyimides indicated either strong intermolecular interactions or good packing ability. Therefore, the large differences in solubility between the **5** and **6** series were attributed to the bulky CF_3 groups, which increased the disorder in the chains and hindered dense chain packing, thereby reducing the interchain interactions to enhance solubility. Table 5 shows the solubility of the **5** series polyimides prepared via chemical imidization. The chemical imidization method could yield polyimides with lower chain packing density, which revealed better solubility than that prepared by thermal imidization method. The chemically imidized polyimides of the **5** series, except for **5b**, were readily soluble at room temperature in strongly polar solvents such as NMP, DMAc, and DMF but also in less polar solvents.

Table 2. Inherent Viscosity (η_{inh}) and Molecular Weight Values of the Organosoluble Fluorinated Polyimides Prepared via Chemical Imidization

Polyimide	η_{inh} (dL/g)[a]	M_w[b]	M_n[b]	M_w/M_n
5c	0.60	72,000	48,500	1.48
5d	0.75	61,000	38,000	1.61
5e	0.80	79,500	48,500	1.64
5f	0.81	86,500	52,500	1.65

[a] Measured at a concentration of 0.5 g/dL in DMAc at 30 °C.
[b] Measured by GPC in THF relative to polystyrene standards.

Tensile Properties

All of the **5** series polyimides afforded good-quality and creasable films with a light color. These films were subjected to a tensile test, and their tensile properties are also reported in Table 1. The films exhibited ultimate tensile strengths of 93–115 MPa, elongations to break of 8–15%, and initial moduli of 1.98–2.09 GPa, comparable to those of the **6** series.

X-Ray Diffraction Data

All the polyimides were characterized with WAXD studies. As can be seen from the diffrac-

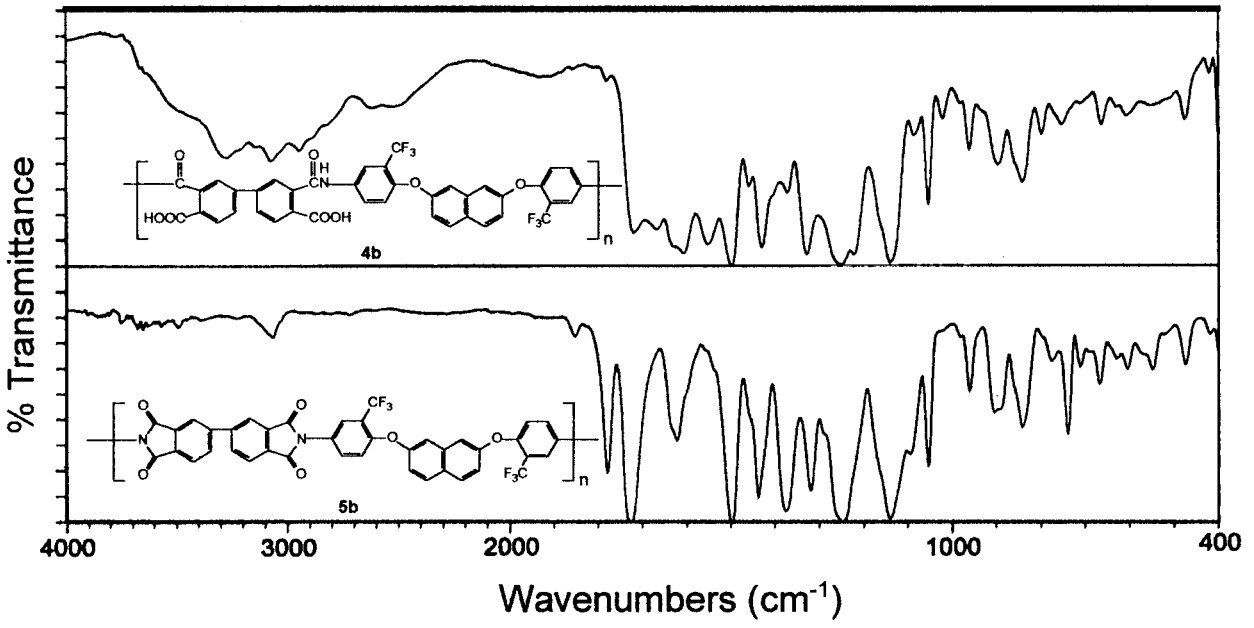

Figure 5. IR spectra (film) of poly(amic acid) **4b** and polyimide **5b**.

tion patterns shown in Figure 6, two of the **6** series polyimides, **6a** and **6c**, displayed a semicrystalline WAXD pattern, whereas all of the others showed amorphous patterns. In contrast to polyimides **6a** and **6c**, the corresponding fluorinated polyimides **5a** and **5c** displayed nearly completely amorphous patterns. All the **5** series polyimides failed to show any crystallinity, apparently because the bulky CF_3 group disrupted the symmetry or dense chain packing leading to highly ordered regions.

Color Intensity and Optical Transparency

The color intensities of the polyimides were elucidated from the yellowness or redness indices observed with a Macbeth color-eye colorimeter. The results shown in Table 6 indicate that the **5** series fluorinated polyimides generally showed a lower b^* value (a yellowness index) in contrast with the corresponding **6** polyimides. Moreover, thin films were measured for optical transparency with UV–vis spectroscopy. Figure 7 depicts the UV–vis spectra of the typical polyimide films, and the cutoff wavelengths (λ_0) from the UV–vis spectra are listed in Table 6. Consistent with the results obtained from colorimeter, all the fluorinated polyimides revealed a lower λ_0 value than their respective CF_3-free analogues. The films from the fluorine-containing polyimides **5** exhibited higher percentage transmittance values ($> 80\%$) than those of films from polyimides **6**. 6FDA and ODPA produced fairly transparent and almost colorless polyimide films in contrast to other dianhydrides, and these were attributed to

Table 3. Elemental Analysis of the Fluorinated Polyimides Prepared via Thermal Imidization

Polyimide	Formula of the Repeat Unit (Formula Weight)	C (%)		H (%)		N (%)	
		Calcd.	Found	Calcd.	Found	Calcd.	Found
5a	$C_{34}H_{14}F_6N_2O_6$ (660.49)	61.83	61.27	2.14	2.05	4.24	4.07
5b	$C_{40}H_{18}F_6N_2O_6$ (736.11)	65.23	64.47	2.46	2.27	3.80	3.94
5c	$C_{41}H_{18}F_6N_2O_7$ (764.10)	64.41	64.01	2.37	2.23	3.66	3.60
5d	$C_{40}H_{18}F_6N_2O_7$ (752.58)	63.84	63.60	2.41	2.26	3.72	3.74
5e	$C_{40}H_{18}F_6N_2O_8S$ (800.64)	60.00	59.55	2.27	2.09	3.50	3.58
5f	$C_{43}H_{18}F_{12}N_2O_6$ (886.61)	58.25	57.89	2.05	2.03	3.16	3.15

Table 4. Solubility Behavior of the Polyimides Prepared via Thermal Imidization[a]

Solvent	Polyimide **5a** Cured at		Polyimide **5b** Cured at		Polyimide **5c** Cured at		Polyimide **5d** Cured at		Polyimide **5e** Cured at		Polyimide **5f** Cured at	
	250 °C	300 °C	250 °C	300 °C	250 °C	300 °C	250 °C	300 °C	250 °C	300 °C	250 °C	300 °C
NMP	+ (−)	+	+h (−)	−	+h (−)	+h	+ (−)	+h	+ (+h)	+h	+ (+h)	+
DMAc	+ (−)	+	− (−)	−	+h (−)	−	+ (−)	+	+ (−)	+	+ (+h)	+
DMF	+ (−)	+	− (−)	−	+h (−)	−	+ (−)	+	+ (−)	+	+ (+)	+
DMSO	+h (−)	+h	− (−)	−	+h (−)	+h	+h (−)	+h	+h (−)	+	+h (+h)	+h
m-Cresol	+h (−)	−	+h (+h)	−	+h (−)	−	+ (+h)	+h	+ (+h)	+h	+h (+h)	+h
2-Chlorophenol	+h (−)	+h	+h (−)	−	+h (−)	−	+ (+h)	+h	+ (+h)	+h	+ (+)	+
THF	− (−)	−	− (−)	−	− (−)	−	+ (−)	+h	+ (−)	+h	+ (+h)	+
1,4-Dioxane	− (−)	−	− (−)	−	− (−)	−	+h (−)	+h	+ (−)	+h	+ (+h)	+h
Dichloromethane	− (−)	−	− (−)	−	− (−)	−	+ (−)	+	+h (−)	+h	+ (+)	+
Acetone	− (−)	−	− (−)	−	− (−)	−	+h (−)	−	− (−)	−	+ (−)	+

[a] The solubility was determined with 10-mg samples in 1 mL of stirred solvent. + = soluble at room temperature; +h = soluble on heating at 100 °C or the boiling temperature of the solvent; − = insoluble even on heating. Data in parentheses are those of the structurally similar **6** polyimides without the 3F groups.

Table 5. Solubility Behavior of the Fluorinated Polyimides Prepared via Chemical Imidization[a]

Solvent	Polyimide **5a**	**5b**	**5c**	**5d**	**5e**	**5f**
NMP	+	−	+	+	+	+
DMAc	+	−	+	+	+	+
DMF	+	−	+	+	+	+
DMSO	+h	−	+	+	+	+
m-Cresol	−	−	+	+	+	+
2-Chlorophenol	+	−	+	+	+	+
THF	−	−	+	+	+	+
1,4-Dioxane	−	−	+	+	+	+
Dichloromethane	−	−	+	+	+h	+
Acetone	−	−	−	+h	+	+

[a] The solubility was determined with 10-mg samples in 1 mL of stirred solvent. + = soluble at room temperature; +h = soluble on heating at 100 °C or the boiling temperature; − = insoluble even on heating.

the reduction of the intermolecular charge-transfer complex (CTC) between alternating electron-donor (diamine) and electron-acceptor (dianhydride) moieties. The light colors of the polyimides with the CF_3 groups in their diamine moieties could be explained by the decreased intermolecular interactions. The bulky and electron-withdrawing CF_3 group in diamine **2** was effective in decreasing CTC formation between polymer chains through steric hindrance and the inductive effect (by decreasing the electron-donating property of diamine moieties). A secondary positive effect of the CF_3 groups on the film transparency was the weakened intermolecular cohesive force due to the lower polarizability of the C—F bond. The decrease in intermolecular CTC formation was understandable also from the significant solubility of the polyimides prepared from CF_3-diamine **2**.

Thermal Properties

The thermal properties of the polyimides were determined with DSC, TMA, and TGA (Table 7). DSC experiments were conducted at a heating rate of 20 °C/min in nitrogen. Rapid cooling from 400 °C to room temperature produced predominantly amorphous samples, so the T_g's of almost all the polyimides could easily be read in the subsequent heating traces. The semicrystalline polyimide **6c** exhibited a well-defined melting endotherm around 394 °C on the first DSC heating trace, whereas the **5c** counterpart showed no

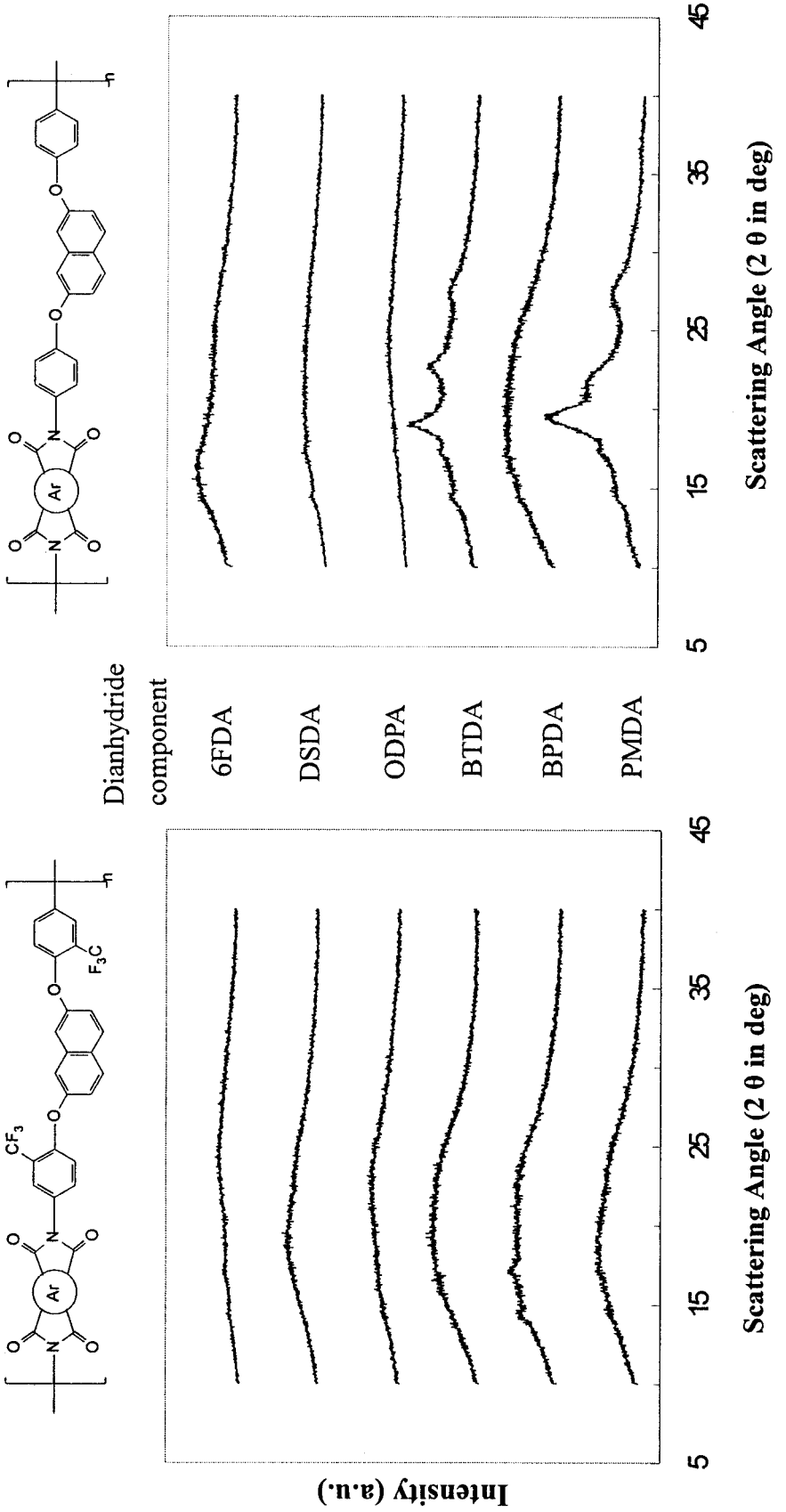

Figure 6. WAXD patterns of the **5** (left) and **6** (right) series polyimides.

Table 6. Color Coordinates and λ_0 Values from UV–vis Spectra for Both **5** and **6** Series Polyimide Films[a]

Polymer	Film Thickness (μm)	a^*	b^*	L^*	λ_0 (nm)
Paper		0.04	0.01	100	
5a	93	−5.31	53.16	89.49	439
5b	85	−2.12	34.47	86.16	415
5c	83	−3.76	41.29	88.04	424
5d	84	−3.74	20.32	94.81	383
5e	84	−10.14	39.42	91.70	407
5f	88	−3.95	13.03	96.41	377
6a	87	23.84	73.17	67.00	465
6b	74	1.42	50.17	76.06	441
6c	82	14.26	64.17	75.25	469
6d	72	−3.99	32.82	88.43	397
6e	79	−0.12	62.02	80.48	432
6f	87	−6.51	30.28	90.84	397

[a] The color parameters were calculated according to a CIE LAB equation with paper as a standard. L^* is lightness; 100 means white, and 0 implies black. A positive a^* values means red, whereas a negative a^* value indicates green. A positive b^* value means yellow, whereas a negative b^* value implies blue.

melting endotherms. Although polyimide **6a** revealed a somewhat crystalline WAXD pattern, it did not show discernible melting endotherms on the DSC curve before 500 °C, possibly because of a high melting temperature. The T_g values of the **5** series polyimides ranged from 244 to 297 °C. The decreasing order of T_g generally correlated with that of the chain flexibility. Therefore, polyimide **5d**, obtained from ODPA, showed the lowest T_g (244 °C) because of the presence of a flexible ether linkage between the phthalimide units, and the highest T_g of 297 °C was observed for polyimide **5a** derived from PMDA. DSC observed no T_g value for polyimide **6a**, possibly because of the high level of crystallinity and the rigid nature of the backbone. The range of T_g values for other **6** series polyimides (**6b–6f**) was 252–289 °C. Slightly lower T_g's for the **5a–5f** series in comparison with the **6a–6f** series might be a result of reduced interactions and poor packing due to the bulky pendant CF_3 groups. The T_s's (or apparent T_g's) of the polyimide films were determined by the TMA method with a loaded penetration probe. They were read from the onset temperature of the probe displacement on the TMA trace. As a representative example, the TMA trace of polyimide **5a** is illustrated in Figure 8. As can be seen from Table 7, in most cases, the T_s values obtained by TMA were comparable to the T_g values measured by the DSC experiments. The trend of T_s variation with the chain stiffness was similar to that of

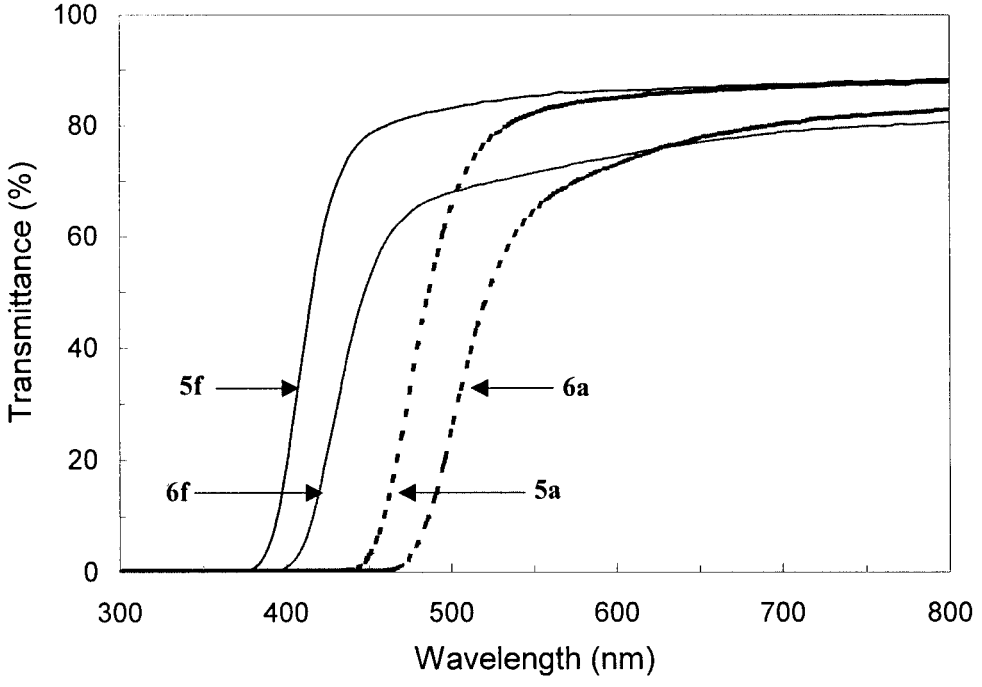

Figure 7. Transmission UV–vis absorption spectra of some polyimide films (87–93 μm thick).

Table 7. Thermal Behavior Data of the Polyimides

Polymer	T_g (°C)[a]	T_s (°C)[b]	T_d at 5% weight Loss (°C)[a]		T_d at 10% weight Loss (°C)[c]		Char Yield (%)[d]
			In N_2	In Air	In N_2	In Air	
5a	297	294	603	593	634	626	61
5b	271	268	616	600	643	631	62
5c	254	234	614	598	643	633	61
5d	244	230	634	607	656	637	62
5e	271	254	555	562	591	593	57
5f	264	244	584	574	607	600	55
6a	—[e]	292	627	610	644	630	67
6b	272	265	610	602	639	632	70
6c	265 (394)[f]	261	608	596	630	627	64
6d	252	251	619	604	637	632	65
6e	289	285	536	559	566	594	56
6f	280	279	582	577	606	603	62

[a] Midpoint temperature of the baseline shift on the second DSC heating trace (rate = 20 °C/min) of the sample after quenching from 400 °C.
[b] Softening temperature measured by TMA (penetration method) with a constant applied load of 10 mN at a heating rate of 10 °C/min. The film samples were heated at 300 °C for 30 min before the TMA experiments.
[c] Decomposition temperatures recorded by TGA at a heating rate of 20 °C/min.
[d] Residual weight percentage at 800 °C in nitrogen.
[e] No discernible transition.
[f] Peak top temperature of the melting endotherm on the first DSC heating trace.

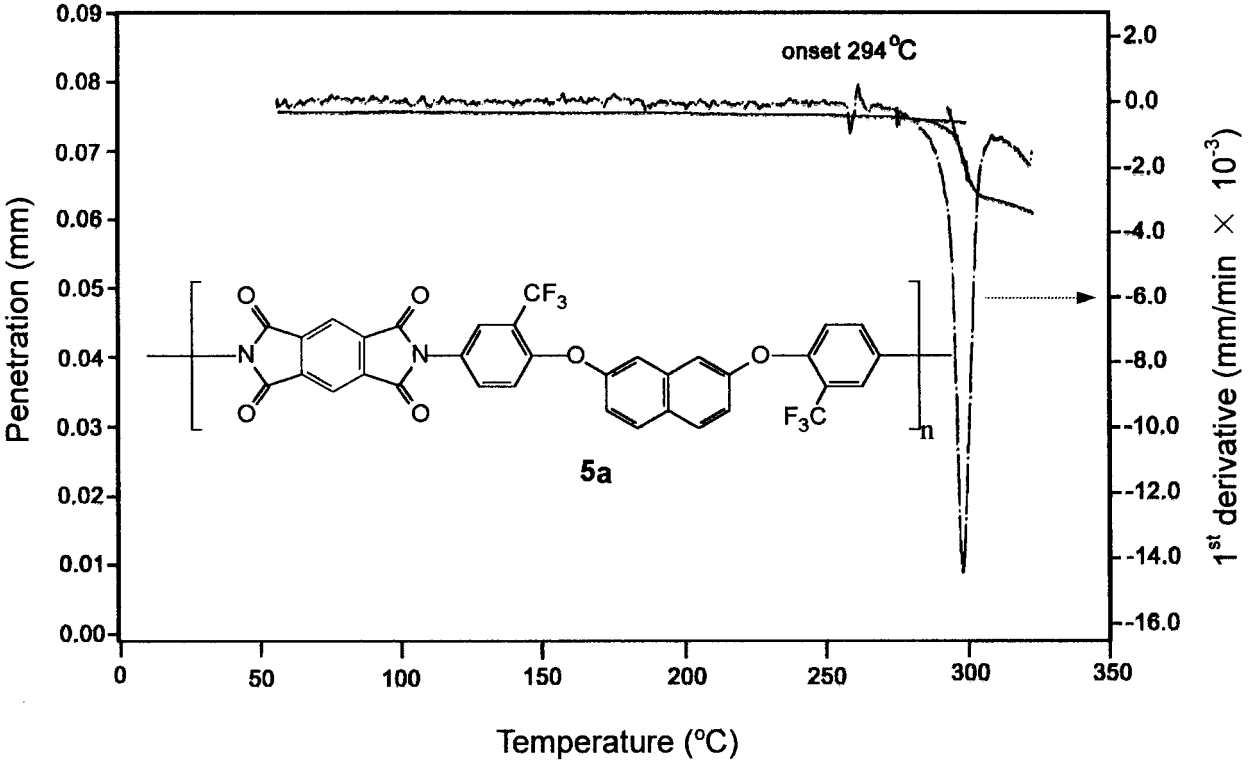

Figure 8. Typical TMA thermogram for polyimide **5a** (heating rate = 10 °C/min, applied force = 10 mN).

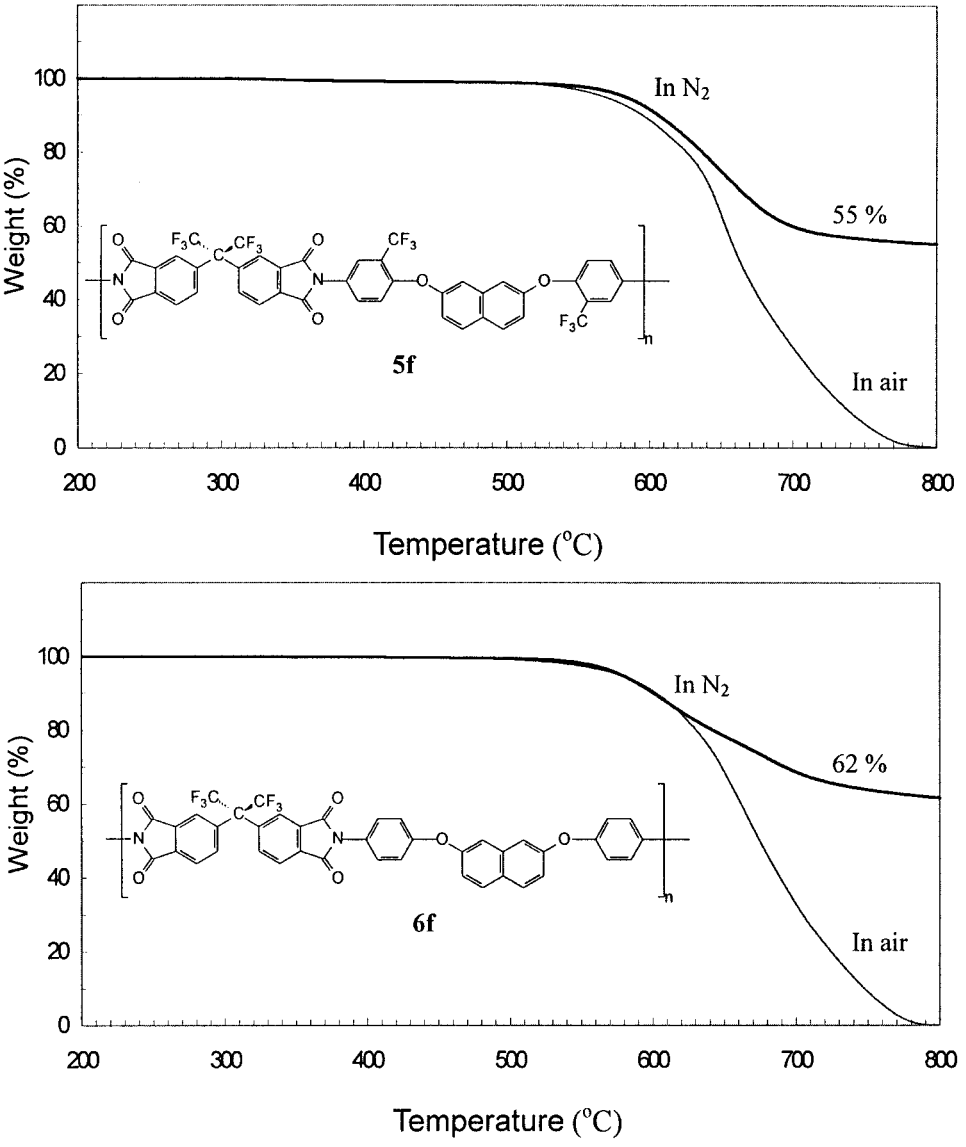

Figure 9. TGA thermograms of polyimides **5f** and **6f** at a heating rate of 20 °C/min.

T_g observed in the DSC measurements. In some cases, such as polyimides **5c–5f**, the T_s values were lower than the T_g values by a larger difference of 14–20 °C. The relatively lower T_s values for these polyimides may indicate that they exhibited a higher degree of plasticity near T_g because of the increased free volume caused by the bulky CF_3 groups.

The thermal stability of the polyimides was evaluated by TGA measurements in both air and nitrogen atmospheres. Typical TGA curves for polyimides **5f** and **6f** are reproduced in Figure 9. The decomposition temperatures (T_d) at 5% and 10% weight losses in nitrogen and air atmospheres were determined from the original TGA thermograms and are given in Table 7. The T_d's at a 10% weight loss of the fluorinated polyimides (**5a–5f**) in nitrogen and air stayed in the ranges of 591–656 and 593–637 °C, respectively. They left more than a 55% char yield at 800 °C in nitrogen. The TGA data indicated that these polyimides had fairly high thermal stability comparable with that of polyimides **6a–6f** derived from nonfluorinated 2,7-BAPON.

Dielectric Constants and Moisture Absorption

The measurements of the dielectric constants were performed between gold layers: the polyimide film was dried carefully, and a thin gold layer

Table 8. Moisture Absorption and Dielectric Constants of the Polyimides

Polymer Code	Film Thickness (μm)	Fluorine Content (%)	Moisture Absorption (%)	Dielectric Constant (Dry)	
				10 kHz	1 MHz
5a	90	17.6	0.51	3.17	3.16
5b	85	15.5	0.63	3.13	3.10
5c	83	14.9	0.66	3.27	3.31
5d	84	14.2	0.57	2.93	2.90
5e	84	15.2	0.60	3.16	3.16
5f	88	25.7	0.29	2.52	2.47
6a	85	0	0.47	3.50	3.44
6b	74	0	0.75	3.32	3.22
6c	82	0	0.88	3.27	3.20
6d	72	0	0.75	3.06	3.06
6e	79	0	0.63	3.52	3.43
6f	87	15.2	0.38	2.68	2.59

was vacuum-deposited onto both surfaces of the polymer film. This procedure excluded any contact problems. As shown in Table 8, polyimides **5a**–**5f** revealed lower dielectric constants (2.52–3.27 at 10 kHz) than analogous polyimides **6a**–**6f** (2.68–3.52 at 10 kHz). The decreased dielectric constants might be partly attributable to the bulky CF_3 groups, which resulted in less efficient chain packing and increased free volume. In addition, the strong electronegativity of fluorine resulted in permanent dipole moments of the CF_3 groups, thereby reducing the dielectric constant. Table 8 also presents the moisture absorption of the polyimides, which ranged from 0.29 to 0.66%. In comparison, most of the polyimides **5a**–**5f** exhibited lower moisture absorption than the corresponding homologue **6a**–**6f** polyimide films. Polyimide **5f** exhibited the lowest moisture absorption because of the higher fluorine content in the repeat unit. Therefore, the 6FDA-derived polyimide **5f** exhibited the lowest dielectric constant of 2.52 at 10 kHz because of the higher free volume and hydrophobicity.

CONCLUSIONS

A novel fluorinated diamine monomer (**2**) was synthesized via a straightforward, high-yielding, two-step procedure including the Williamson etherification reaction. A series of novel fluorinated polyimides were obtained from the CF_3-substituted bis(ether amine) with various aromatic dianhydrides by two-step thermal or chemical imidization methods. The resulting polyimides were characterized by high solubility, good film-forming capability, high optical transparency, excellent thermal stability, moderate to high T_g's (244–297 °C), and low dielectric constants. Therefore, this series of polyimides demonstrated a good combination of properties and processability.

The authors are grateful to the National Science Council of the Republic of China for its financial support of this work (NSC 91-2216-E-036-007).

REFERENCES AND NOTES

1. Polyimides; Wilson, D.; Stenzenberger, H. D.; Hergenrother, P. M., Eds.; Blackie: Glasgow, 1990.
2. Eastmond, G. C.; Paprotny, J. React Funct Polym 1996, 30, 27.
3. Eastmond, G. C.; Paprotny, J. Eur Polym J 1999, 35, 2097.
4. Imai, Y. React Funct Polym 1996, 30, 3.
5. Ayala, D.; Lozano, A. E.; de Abajo, J.; de la Campa, J. G. J Polym Sci Part A: Polym Chem 1999, 37, 805.
6. Li, F.; Ge, J. J.; Honigfort, P. S.; Fang, S.; Chen, J.-C.; Harris, F. W.; Cheng, S. Z. D. Polymer 1999, 40, 4987.
7. Liou, G.-S.; Maruyama, M.; Kakimoto, M.; Imai, Y. J Polym Sci Part A: Polym Chem 1998, 36, 2021.
8. Hsiao, S.-H.; Yang, C.-P.; Chu, K.-Y. Macromolecules 1997, 30, 165.
9. Yang, C.-P.; Hsiao, S.-H.; Yang, H.-W. Macromol Chem Phys 2000, 201, 409.

10. Myung, B. Y.; Kim, J. J.; Yoon, T. H. J Polym Sci Part A: Polym Chem 2002, 40, 4217.
11. Yang, C.-P.; Chen, W.-T. Macromolecules 1993, 26, 4865.
12. Tamai, S.; Yamaguchi, A.; Ohta, M. Polymer 1996, 37, 3683.
13. Li, F.; Fang, S.; Ge, J. J.; Honigfort, P. S.; Chen, J.-C.; Harris, F. W.; Cheng, S. Z. D. Polymer 1999, 40, 4571.
14. Spiliopoulos, I. K.; Mikroyannidis, J. A. Macromolecules 1998, 31, 515.
15. Xu, J.; He, C.; Chung, T.-S. J Polym Sci Part A: Polym Chem 2001, 39, 2998.
16. Jeong, K. U.; Jo, Y. J.; Yoon, T. H. J Polym Sci Part A: Polym Chem 2001, 39, 3335.
17. Liu, J. G.; Li, Z. X.; Wu, J. T.; Zhou, H. W.; Wang, F. S.; Yang, S. Y. J Polym Sci Part A: Polym Chem 2002, 40, 1583.
18. Maier, G. Prog Polym Sci 2001, 26, 3.
19. Chern, Y.-T.; Shiue, H.-C. Macromolecules 1997, 30, 4646.
20. Chern, Y.-T.; Shiue, H.-C. Macromol Chem Phys 1998, 199, 963.
21. Chern, Y.-T.; Shiue, H.-C. Macromolecules 1997, 30, 5766.
22. Chern, Y.-T. Macromolecules 1998, 31, 5837.
23. Sasaki, S.; Nishi, S. In Polyimides: Fundamentals and Applications; Ghosh, M. K.; Mittal, K. L., Eds.; Marcel Dekker: New York, 1996; pp 71–120; see also references therein.
24. Hougham, G. In Fluoropolymers: Synthesis and Properties; Hougham, G.; Cassidy, P. E.; Johns, K.; Davidson, T., Eds.; Kluwer Academic/Plenum: New York, 1999; Vol. 2, pp 233–276.
25. Ando, S.; Matsuura, T.; Sasaki, S. In Fluoropolymers: Synthesis and Properties; Hougham, G.; Cassidy, P. E.; Johns, K.; Davidson, T., Eds.; Kluwer Academic/Plenum: New York, 1999; Vol. 2, pp 277–303.
26. Matsuura, T.; Ando, S.; Sasaki, S. In Fluoropolymers: Synthesis and Properties; Hougham, G.; Cassidy, P. E.; Johns, K.; Davidson, T., Eds..; Kluwer Academic/Plenum: New York, 1999; Vol. 2, pp 305–350.
27. Harris, F. W.; Li, F.; Cheng, S. Z. D. In Fluoropolymers: Synthesis and Properties; Hougham, G.; Cassidy, P. E.; Johns, K.; Davidson, T., Eds.; Kluwer Academic/Plenum: New York, 1999; Vol. 2, pp 351–370.
28. Takashi, K.; Atsushi, S.; Shoji, T. (Mitsui Chemistry Industry Co.). Jpn Kokai Tokyo Koho JP 2000 297,067; Chem Abstr 2000, 133, 322563h.
29. Takashi, K.; Atsushi, S.; Shoji, T. (Mitsui Chemistry Industry Co.). Jpn Kokai Tokyo Koho JP 2000 297,153; Chem Abstr 2000, 133, 322280p.
30. Takashi, K.; Atsushi, S.; Shoji, T. (Mitsui Chemistry Industry Co.). Jpn Kokai Tokyo Koho JP 2000 297,154; Chem Abstr 2000, 133, 310300g.
31. Xie, K.; Liu, J. G.; Zhou, H. W.; Zhang, S. Y.; He, M. H.; Yang, S. Y. Polymer 2001, 42, 7267.
32. Xie, K.; Zhang, S. Y.; Liu, J. G.; He, M. H.; Yang, S. Y. J Polym Sci Part A: Polym Chem 2001, 39, 2581.
33. Yang, C.-P.; Hsiao, S.-H.; Hsu, M.-F. J Polym Sci Part A: Polym Chem 2002, 40, 524.
34. Yang, C.-P.; Hsiao, S.-H.; Chen, K.-H. Polymer 2002, 43, 5059.
35. Zhou, H. W.; Liu, J. G.; Qian, Z. G.; Zhang, S. Y.; Yang, S. Y. J Polym Sci Part A: Polym Chem 2001, 39, 2404.
36. Liu, J. G.; He, M. H.; Li, Z. X.; Qian, Z. G.; Wang, F. S.; Yang, S. Y. J Polym Sci Part A: Polym Chem 2002, 40, 1572.
37. Liu, J. G.; He, M. H.; Zhou, H. W.; Qian, Z. G.; Wang, F. S.; Yang, S. Y. J Polym Sci Part A: Polym Chem 2002, 40, 110.
38. Banerjee, S.; Madhra, M. K.; Salunke, A. K.; Maier, G. J Polym Sci Part A: Polym Chem 2002, 40, 1016.
39. Yang, C.-P.; Chen, W.-T. Macromol Chem Phys 1993, 194, 3061.
40. Yang, C.-P.; Chen, W.-T. Macromolecules 1993, 26, 4865.
41. Yang, C.-P.; Chen, W.-T. J Polym Sci Part A: Polym Chem 1993, 31, 2799.
42. Yang, C.-P.; Hsiao, S.-H.; Jang, C.-C. J Polym Sci Part A: Polym Chem 1995, 33, 1487.
43. Yang, C.-P.; Chen, J.-A. Polym J 1998, 30, 571.